

Article

Heat Resistance of Centrifugally Cast Tubes Made of 32%Cr-43%Ni Refractory Alloy and Its Welded Joints at Temperatures up to 1150 °C

Sergey N. Petrov *, Irina P. Popova, Alina V. Tsemenko, Ekaterina V. Zabavicheva, Julia A. Belikova and Yury S. Puzikov

National Research Center “Kurchatov Institute”—CRISM “Prometey”, St. Petersburg 191015, Russia;
ip2365411@gmail.com (I.P.P.); alina-pv@mail.ru (A.V.T.); svyatyscheva.ek@yandex.ru (E.V.Z.);
belikjul@yandex.ru (J.A.B.); y.-zapan@list.ru (Y.S.P.)

* Corresponding author. E-mail: petrov.epma@mail.ru (S.N.P.)

Received: 17 July 2025; Accepted: 4 September 2025; Available online: 15 September 2025

ABSTRACT: The results of microstructural analysis, short-term and long-term strength tests of modified sparingly alloyed refractory alloy of 32%Cr-43%Ni and its welded joints are presented. A quantitative analysis of the dispersed phases in the initial state and after long-term strength tests has been carried out. It is shown that the network of carbide-intermetallic precipitates persists after long-term strength tests at a temperature of 1150 °C. This ensures the ability of the developed alloy and its welded joints to withstand high-temperature creep for a long time. It has been established that after long-term strength tests at a temperature of 1150 °C, niobium carbide particles present in the base metal and weld metal are almost completely transformed into an intermetallic phase based on Cr-Ni-Si-Nb-N. The penetration of atmospheric nitrogen into the metal stimulates this process.

Keywords: Heat-resistant alloy; Long-term strength; Microstructure; Centrifugal cast tubes; Carbides



© 2025 The authors. This is an open access article under the Creative Commons Attribution 4.0 International License (<https://creativecommons.org/licenses/by/4.0/>).

1. Introduction

SRT-6 coils manufactured by Schmidt+Clemens GmbH (Lindlar, Germany) and Kubota Corp. (Osaka, Japan) are used in petrochemical industry enterprises in hydrocarbon pyrolysis plants. The high-temperature part of coils is made of centrifugal casting tubes manufactured from base composition of 35%Cr-45%Ni alloy. The maximum operating temperature of the reaction tubes is 1125 °C, and the warranty period of the coil is approximately 50 thousand hours. Reaction coils are manufactured using welding from tubes of 3.0 to 6.0 m in length. Welding material for pyrolysis furnaces of a new generation must have good resistance to high-temperature creep and corrosion, have a chemical composition and a coefficient of thermal expansion close to the base metal [1]. Previous studies have revealed in the welds of the basic composition 35%Cr-45%Ni a framework of precipitations along the boundaries of dendritic cells, which has structural stability under prolonged high-temperature loading [2,3]. During long-term strength tests, the predominant fracture of samples was recorded in the heat-affected zone (HAZ) near the fusion boundary. Analysis of changes in phase composition revealed a significant increase in nitrogen-containing phases in the HAZ. It is established that both in the base metal and in the welded joint, there is an almost complete transformation of niobium carbide into an intermetallic compound based on Cr-Ni-Si-Nb-N under the influence of atmospheric nitrogen penetrating the metal. The negative effect of nitrogen penetration on the heat resistance of the base metal at a temperature of 1100 due to the depletion of the solid solution of austenite during the formation of chromium carbonitrides has already been noted in [4]. This problem is still poorly covered in the existing literature. The paper considers the test results and analyzes structural and phase changes in the metal of welded joints in order to identify the factors causing this type of failure.

2. Materials and Methods

Studies of the microstructure, phase composition, and mechanical properties were performed on the base metal of centrifugal cast tubes $\varnothing 118 \times 14$ mm made of 32%Cr-43%Ni modified alloy and welded joints made by the argon-arc method using Thermanit 35/45 Nb filler rods $\varnothing 2.4$ mm (Boehler, Kapfenberg, Austria). The content of nickel and niobium in the base metal has been reduced, and microalloying with molybdenum and niobium has been added. The composition of the studied materials obtained using atomic emission spectroscopy is shown in Table 1.

Table 1. Chemical composition of metal tubes and welds.

Material	C	S	P	Si	Mn	Cr	Ni	Nb	Mo	W
Mass Fraction, %										
tubes	0.49	0.008	0.013	1.70	1.60	34.3	42.8	0.85	0.48	0.69
welds	0.42	0.001	0.009	1.49	1.0	35.5	45.2	0.74	<0.1	-

Short-term mechanical properties at room temperatures in air are determined using Zwick Z050 type BT1-FR050TEW.A1K equipment (ZwickRoel, Ulm, Germany) in accordance with GOST 1497-2023 requirements. Long-term strength tests were carried out in accordance with the requirements of GOST 10145-81 at a temperature of 1150 °C in air using the upgraded AIMA-5-1 testing machine (Tochpribor, Ivanovo, Russia), using the direct loading method with recording of the relative elongation of the samples. Post-welding heat treatment was not used to simulate the actual condition of mounting welded joints in the structures of large-sized pyrolysis columns. The microstructure of the metal and element analysis of the dispersed phases were investigated using a Vega II LM scanning electron microscope (TESCAN, Brno, Czech) equipped with an X-Max-50 energy dispersion spectrometer (Oxford Instr., Abingdon, Great Britain). Element analysis of different disperse phases was proceeded at electron energy of 20 keV and probe current about 0.7 nA. In this case, conditions provide a detection limit about 0.05 mass. % for elements with atomic number Z more than 11 and about 1 mass. % for nitrogen. The phase composition of the samples after long-term strength tests at the same temperature and stress was estimated by the proportion of the area occupied in the image in backscattered electrons by one phase or another. The separation of phases were carried out by digital image processing with the allocation of contrast ranges characteristic of the analyzed phase [5]. Sections for microstructural research are prepared in the plane of the sample axis after long-term strength tests. The microstructure of the base and welded metal was analyzed on the working part of the samples at the same temperature and at the same stress. The time to failure at 6 MPa and temperature of 1150 °C for base and welded metal is noticeably different, 405 h for the former and 277 h for the latter. Different long-term strengths are well-known facts for heat-resistant materials and their welded joints. The microstructure of the HAZ near the fracture site was analyzed.

3. Results

3.1. The Short-Term Mechanical Properties

The values of the short-term mechanical properties of the base metal and welded tube joints at room temperature in air are given in Table 2. The guaranteed values of the mechanical characteristics are calculated with a probability of 95%. The strength properties (yield strength $R_p 0.2$ and tensile strength R_m) of the weld tube joints exceed those of the base metal, while the plastic characteristics (elongation after rupture δ and the relative narrowing of the cross-section after the break Ψ) are slightly lower. Minimum values of the modified alloy 32%Cr-43%Ni refractory alloy mechanical properties exceed the corresponding values of its foreign counterparts, KHR45A and ET 45 Micro [4].

Table 2. Mechanical properties at room temperature.

Material	R_m , MPa	$R_p 0.2$, MPa	δ , %	Ψ , %
welded joint *	605	401	5	3
base metal	562	325	7.8	6.5

* Fracture site—HAZ.

3.2. The Long-Term Strength Properties

Figure 1 shows the creep curves of the welded (a) and base metal (b), obtained at a temperature of 1150 °C by direct loading in air. Solid and dotted lines indicate repeated tests under the same conditions. All three stages of creep are present: the duration of the first stage has been reduced to several hours.

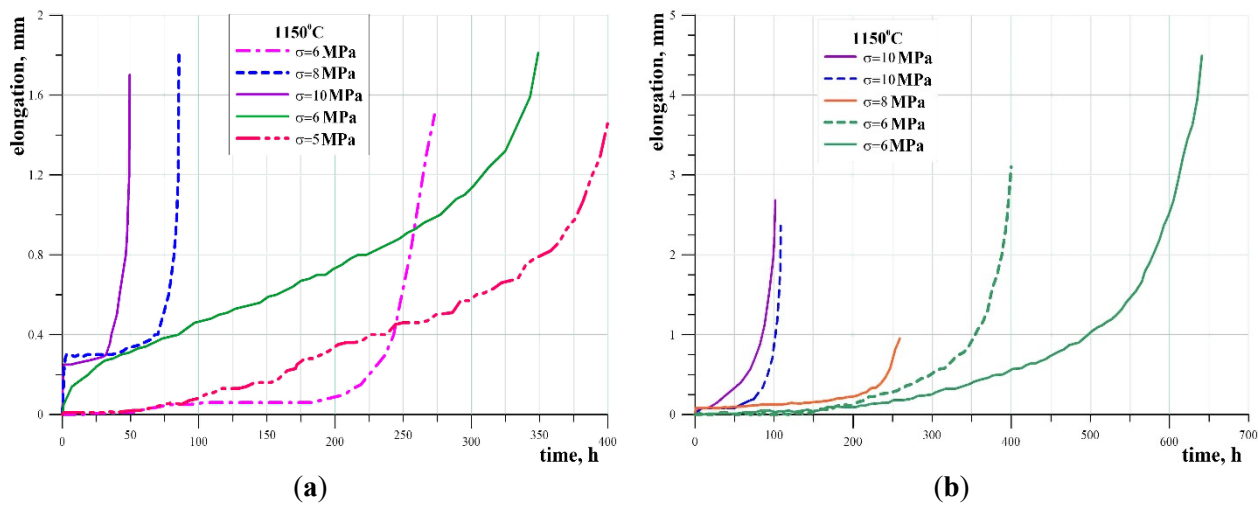


Figure 1. Creep curves of welded tube joints made of 35/45 Nb alloy—(a) and base metal made of 32%Cr-43%Ni alloy—(b) obtained at a temperature of 1150 °C.

Figure 2 shows the long-term strength curves of welded joints of tubes and base metal at a temperature of 1150 °C. Straight lines are an approximation of the experimental data by a power dependence. The equations for the weld metal (1) and (2) for the base metal are an analytical approximation of the experimental dependences. (R^2 is the coefficient of determination, τ is the time to fracture):

$$\sigma = 32.04\tau^{-0.3045}, R^2 = 0.95 \quad (1)$$

$$\sigma = 41.84\tau^{-0.3086}, R^2 = 0.95 \quad (2)$$

The time to fracture of samples from a welded joint at the same stress is approximately two times less than for the base metal. It should be noted that in the tubes of the high-temperature part of pyrolysis plants, the stresses, as a rule, do not exceed 1 MPa. The obtained experimental dependences of long-term strength show that the condition of long-term strength at a temperature of 1150 °C based on 10 thousand hours is fulfilled for the base metal and welded joints (Figure 2).

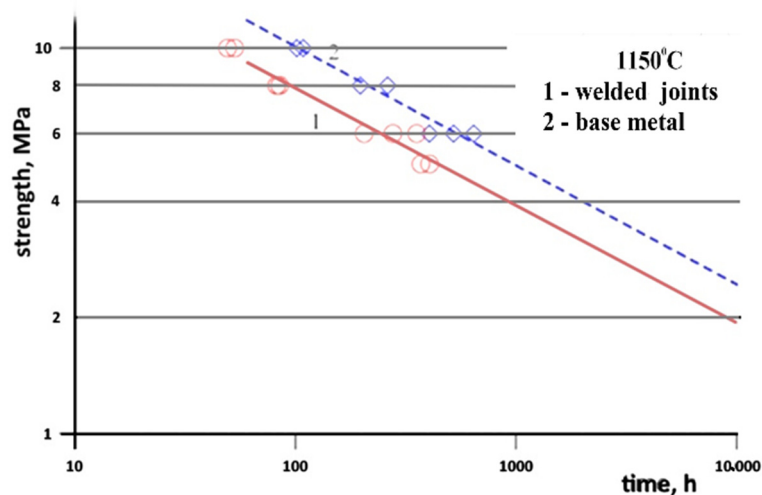


Figure 2. Long-term strength of welded tube joints (1) and base metal (2) at a temperature of 1150 °C.

3.3. Metal Microstructure

Figure 3 shows the microstructure of the 32%Cr-43%Ni alloy in its state of supply. In the backscattered electron image, chromium carbides have a darker contrast compared to the austenitic matrix, whereas niobium carbides have a lighter contrast due to differences in average atomic number. These data are confirmed by studies of the local composition of the observed phases. A quantitative phase analysis based on phase separation by contrast level was performed on a representative series of image fields. Table 3 shows the average values of the volume fraction of dispersed phases of the base metal, the welded metal, and the HAZ in the state of supply and after long-term strength tests.

Table 3. Results of phase analysis of base metal (BM), welded metal (WM) and HAZ.

Phase	BM the State of Supply	WM the State of Supply	BM 1150 °C, 405 h	WM 1150 °C, 277 h	HAZ 1150 °C, 277 h
	Volume Fraction, %				
chromium carbides	5.2 ± 0.3	4.1 ± 0.3	12.3 ± 0.3	12.5 ± 0.3	11.4 ± 0.3
niobium carbides	1.3 ± 0.3	0.8 ± 0.3	-	0.2	0.1
intermetallic phase	-	-	2.7 ± 0.3	0.8 ± 0.3	4.5 ± 0.3

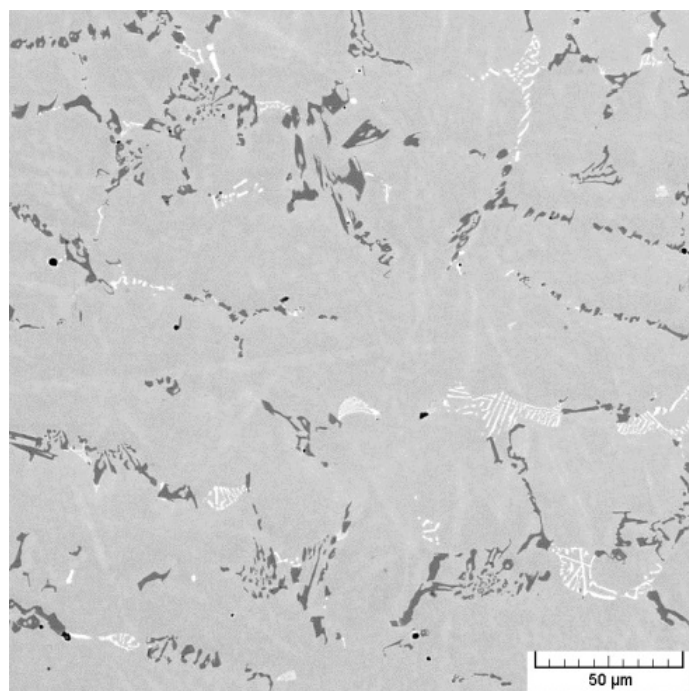


Figure 3. Microstructure of the 32%Cr-43%Ni alloy in its initial state.

In the state of supply, there is a clear boundary between the base metal and the weld material (Figure 4). The cell size of the welded metal is significantly smaller; in addition, the dispersed particles in the welded metal are much smaller than the precipitates in the base metal. The volume fraction of chromium carbides and niobium carbides in the welded metal is significantly less than that of the base metal (Table 3).

The microstructure of the 32%Cr-43%Ni alloy after long-term strength tests at 6 MPa and a temperature of 1150 °C for 405 h is shown in Figure 5. The phase composition has changed significantly compared to the state of supply. Globular chromium carbides of sizes up to 30 microns were detected, and a large number of dispersed chromium carbides of micron and submicron sizes were. No niobium carbides were found in the base metal, whereas they are present in minimal amounts in the welded metal and in the HAZ. Globular intermetallic particles based on Cr-Ni-Si-Nb-N were also detected (Figure 5). The formation of similar intermetallic phases in chromium-iron-nickel alloys after high-temperature exposure at temperatures above 1100 °C was previously noted in [5], as well as in [6,7]. Of particular note is the presence of nitrogen in the composition of the detected phase, which, apparently, stimulates its formation. At the same time, the nitrogen content does not exceed 3.5 mass. %, which is clearly insufficient for the formation of nitride. In this regard, its position in the crystal lattice of the intermetallic compound and its role in stabilizing the identified phase remain unclear. The composition stability of the revealed intermetallic high-temperature phase should

also be noted. Its composition is practically constant after prolonged exposure at a temperature of 1100 °C [4] and after long-term strength tests at a temperature of 1150 °C.

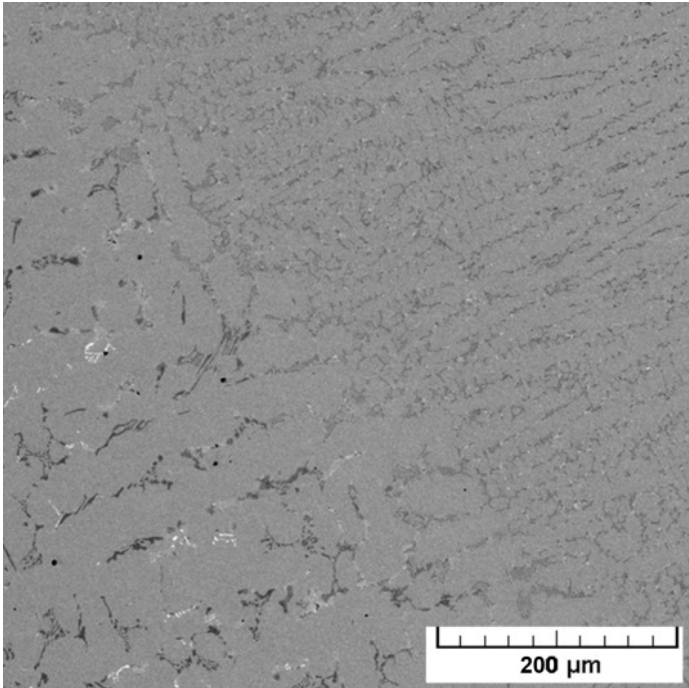
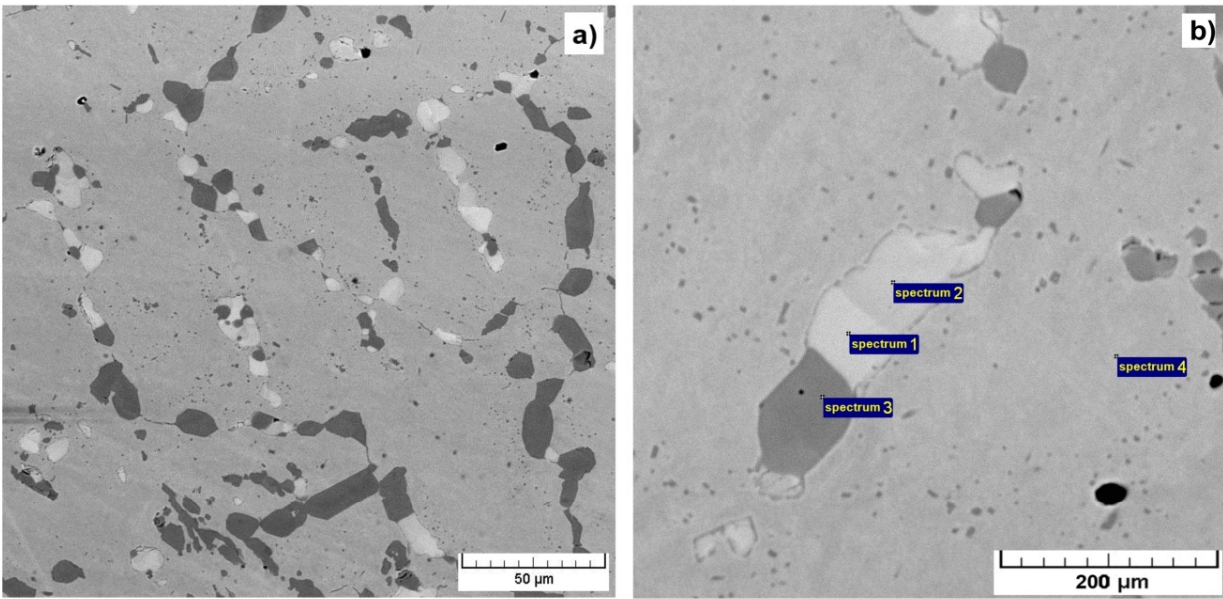


Figure 4. Image of the microstructure at the base metal–joint interface in its initial state.



Spectrum №	Phase	N	Si	Cr	Mn	Fe	Ni	Nb	Mo	W
		Mass fraction, %								
1	intermetallic phase based on Cr-Ni-Si-Nb-N	3.6	7.8	35.9	-	2.4	33.4	17.0	-	-
2		3.0	8.7	35.3	-	2.5	34.1	16.4	-	-
3	chromium carbide		-	84.6	-	5.4	5.6	-	1.4	2.9
4	austenite		1.9	29.2	1.5	19.5	48.0	-	-	-

Figure 5. Microstructure of the base metal after long-term strength tests at 6 MPa for 405 h at a temperature of 1150 °C—(a), the elemental composition of the phases—(b).

Thus, after long-term strength tests at a temperature of 1150 °C, two main types of dispersed phases were revealed in the alloy under investigation—chromium carbides and nitrogen-stabilized Cr-Ni-Si-Nb intermetallic compound. An almost twofold increase in chromium carbides and a complete transformation of niobium carbides into an intermetallic phase based on Cr-Ni-Si-Nb-N were found, as well as coagulation of dispersed phases simultaneously with the formation of a significant number of micron and submicron-sized chromium carbide particles (Figure 5). The differences in the composition of the analyzed particles of the intermetallic phase do not exceed the error in determining the method used (spectra 1 and 2). However, in Figure 5b, obtained in the backscattered electrons mode, there is a noticeable change in the contrast of the analyzed particles. The reason for this is that the contrast of the atomic number (Z-contrast), which should not differ markedly with the same particle composition, is superimposed on the orientation contrast resulting from electron backscattering diffraction at different crystallite orientations.

A sample of welded joint after long-term strength tests at 6 MPa and a temperature of 1150 °C for 277 h fractured along HAZ, as well as a sample after short-term tests at room temperature. In the longitudinal section of the working part of the sample after long-term testing, the fracture line runs at a distance of 100 to 300 microns from the fusion line. A large number of dispersed chromium carbonitride particles are observed in the vicinity of secondary cracks, which indicates an intensive interaction of the metal with atmospheric nitrogen penetrating the opening secondary cracks.

The microstructure of the weld metal after long-term strength tests is shown in Figure 6. Changes in the composition of dispersed precipitates are similar to changes observed after long-term strength tests in the base metal. Unlike the base metal, after long-term strength tests, a small amount of niobium carbide particles of micron and submicron sizes containing a significant amount of titanium were found in the weld metal (Figure 6b). This allows us to conclude that niobium carbides are stabilized by titanium introduced into the weld metal. It should be noted that the weld metal contains significantly less intermetallic phase compared to the base metal with practically the same content of chromium carbides.

Analysis of the phase composition of the HAZ metal revealed the presence of a small amount of niobium carbides, mainly in the center of the intermetallic phase particles, the amount of which is almost 2 times greater than its content in the base metal. At the same time, the content of chromium carbides in the HAZ metal is slightly lower compared to the base metal and the weld metal (Table 3). Apparently, this is due to the partial transformation of chromium carbides into the intermetallic phase, which indicates a more intensive penetration of atmospheric nitrogen into the metal of the HAZ. The arrangement of the intermetallic particles along the cell boundaries of the cast structure (Figure 7) confirms the assumption [4] that its formation can occur not only as a result of the transformation of niobium carbide particles, but also as a result of the transformation of chromium carbide particles into the intermetallic phase of the Cr-Ni-Si-Nb-N system. After long-term strength tests, the presence of niobium carbide particles in the HAZ suggests the diffusion of titanium, which stabilizes niobium carbides, from the weld metal into the HAZ.

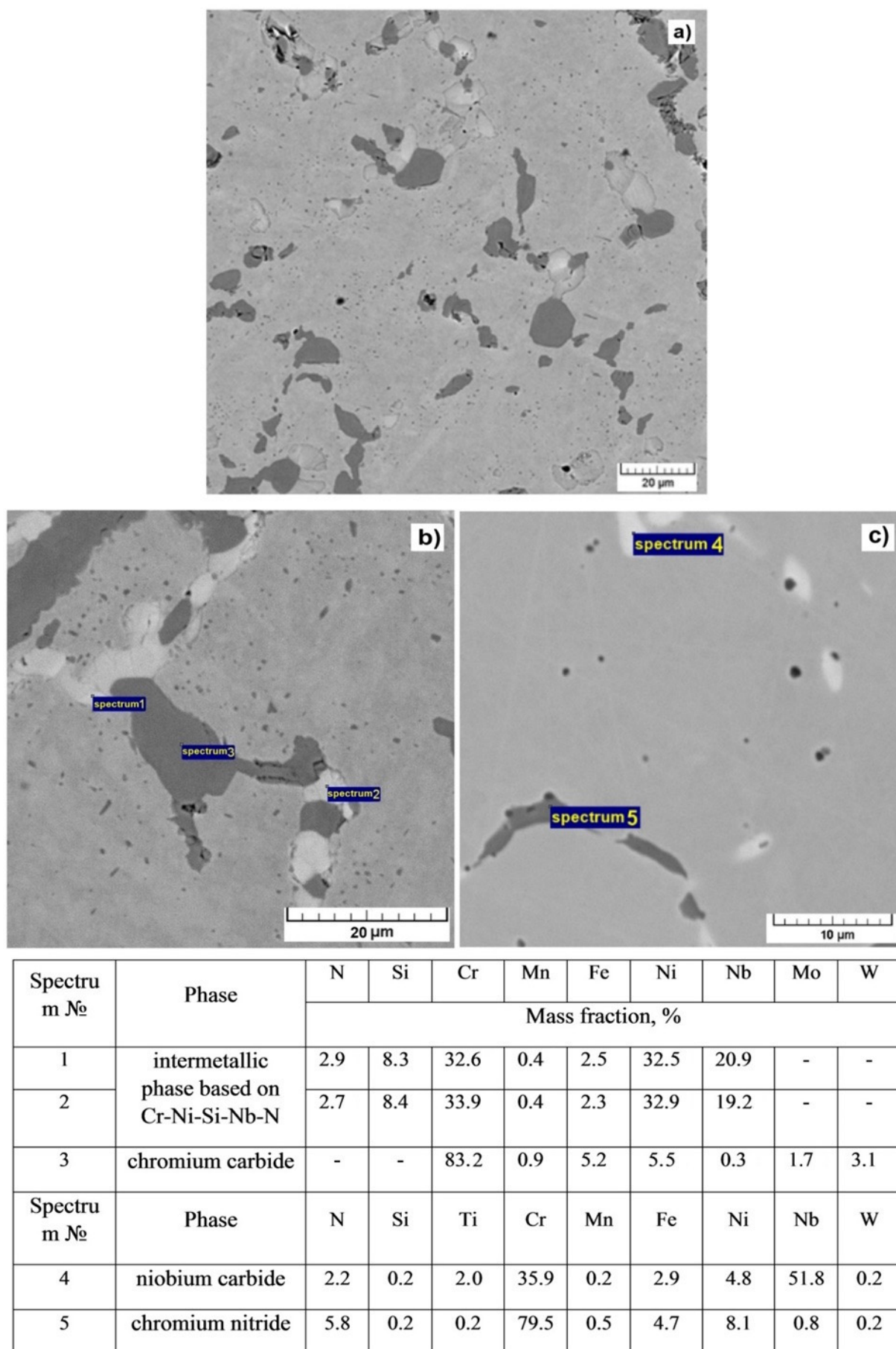


Figure 6. Microstructure of the weld metal after long-term strength tests at 6 MPa for 277 h at a temperature of 1150°C—(a), elemental composition of phases—(b,c).

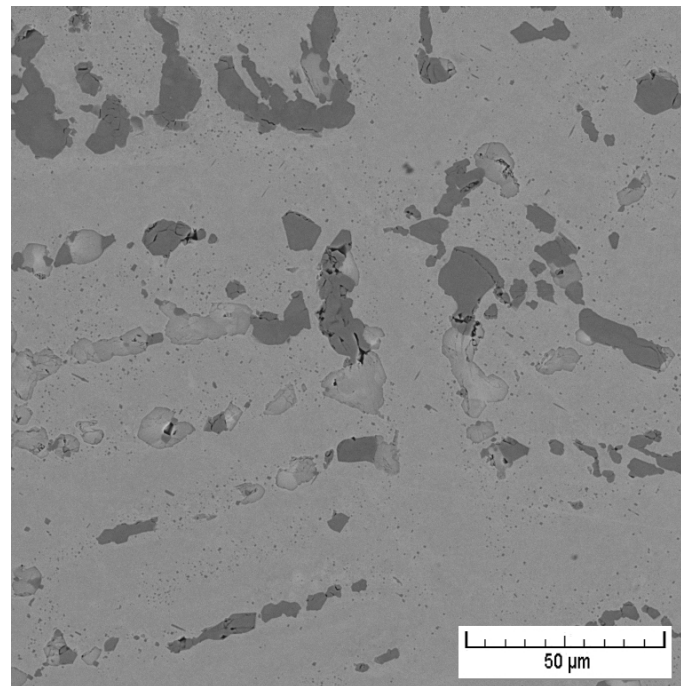


Figure 7. Microstructure of the HAZ metal after long-term strength tests.

4. Discussion

Analysis of the phase composition shows that after long-term strength tests, the volume fraction of chromium carbides increases by more than two times, mainly due to the formation of carbides in the micron and submicron size ranges. This is due to the interaction of chromium with carbon preserved in the dendritic spaces of the solid solution after crystallization, as well as released as a result of the transformation of chromium carbides Cr_7C_3 into Cr_{23}C_6 [8,9] and niobium carbides into intermetallic phases [10–12]. Niobium carbides transform into an intermetallic phase based on Cr-Ni-Si-Nb-N after long-term strength tests at a temperature of 1150 °C. This process, obviously stimulated by the penetration of atmospheric nitrogen into the metal, was also noted in studies of the 45X32H43SB alloy for long-term strength at a temperature of 1100 °C [4], as well as in [6,7]. In work [12], the elemental composition and crystal lattice parameters of the intermetallic phase formed from niobium carbide at a temperature of 1150 °C in the HP40NbTi alloy were analyzed by transmission electron microscopy. It was established that the phase has a cubic face-centered lattice with parameter $a = 1084 \text{ nm}$ (space group $\text{Fd}3\text{m}$) and a composition close to that obtained in the present paper.

The almost complete absence of niobium carbides after long-term strength tests, as well as the presence of nitrogen in the composition of the intermetallic compound, indicates its significant penetration into the metal, both due to diffusion through the surface oxide film and due to penetration through forming microcracks. The morphological and microstructural features of surface protective oxide layers in heat-resistant alloys, as well as the mechanism of their formation, are described in detail in [13–15]. At the same time, the issue of their permeability to nitrogen is practically not covered in the literature. In [4], it was suggested that surface protective oxide layers pass nitrogen into austenite only in dosed amounts during fractures under the influence of creep deformation. Intensive nitrogen penetration occurs at later stages of long-term strength tests, when secondary cracks form under the influence of stress. It has been shown that such cracks are contoured by numerous particles of chromium carbonitrides. This fact was also revealed in the course of this work, although it was not studied in detail. The formation of a large number of carbonitride particles leads to local depletion of the austenite solid solution in chromium and sharp decreases in creep resistance, leading to the intensive opening of secondary cracks.

It should be noted that the maximum content of the intermetallic phase and the minimum content of chromium carbide were found in the HAZ. The tendency to form intermetallides based not only on niobium carbides, but also chromium carbides was noted in [7] and, apparently, the observed ratio of the volume fractions of these phases is a consequence of this process. It can be assumed that a large volume fraction of intermetallic phase particles with a high chromium and nickel content leads to partial dealloying of the austenite solid solution. The consequence of this is a decrease in creep deformation resistance. This is probably one of the reasons for the localization of fractures of welded joint samples in the HAZ after long-term strength tests.

Another reason for the failure of a welded joint specimen along the HAZ is probably the presence of residual tensile stresses directed perpendicular to the axis of the joint. The summation of residual stresses and the applied load at the initial stage of long-term strength tests leads to localization of deformation in the HAZ metal and the formation of microcracks in a less plastic oxide film. This ensures the penetration of atmospheric nitrogen into the metal. Intensive penetration of nitrogen into the HAZ metal is accompanied by the transition of chromium from a solid solution to carbonitrides, which leads to its weakening, and ultimately, to destruction. These processes are the main reason for the lower values of long-term strength of welded joints. In this regard, when designing pyrolysis furnaces, it is important to provide for special measures that prevent deformation of elements made of heat-resistant alloys, such as rigid fixation of vertical parts of radiant coils, sagging horizontal sections due to the small number of supports, etc. Increased attention to the removal of residual stresses in the welded joints of reaction coils made of heat-resistant alloys, as well as the search for ways of protecting metal from atmospheric nitrogen penetration, will make it possible to bring the service life of welded joints closer to that of the base metal.

5. Conclusions

1. It is shown that the long-term strength of the welded joints metal is lower than that of the base metal. The operability of the base metal and the welded joints of the alloy according to the criterion of long-term strength is ensured for a service life of 10 thousand hours.
2. It is shown that the network of carbide-intermetallic precipitates persists after long-term strength tests at a temperature of 1150 °C. This ensures the ability of the developed alloy to resist high-temperature creep.
3. The fracture of the welded joint occurs along the heat-affected zone, both during short-term tests and after long-term strength tests.
4. It has been found that after long-term strength tests, the volume fraction of chromium carbides increases significantly, mainly due to the formation of dispersed secondary chromium carbides.
5. It has been established that after long-term strength tests at a temperature of 1150 °C, the niobium carbide particles present in the base and weld metal are almost completely transformed into an intermetallic phase based on Cr-Ni-Si-Nb-N. Penetration of atmospheric nitrogen into the metal stimulates this process.
6. It is shown that after long-term strength tests at a temperature of 1150 °C, the content of the Cr-Ni-Si-Nb-N-based intermetallic phase in the HAZ metal is approximately twice as high as its content in the base and weld metal. This indicates a more intensive penetration of atmospheric nitrogen into the metal at this site. Localization of deformation in the HAZ at the initial testing stage due to tensile residual welding stresses contributes to the formation of microcracks in the resulting oxide film. It facilitates the penetration of atmospheric nitrogen into the metal in this area.

Acknowledgments

Experimental studies were carried out on the equipment of the Core shared research facilities “Composition, microstructure and properties of structural and functional materials” of the NRC «Kurchatov Institute»—CRISM “Prometey”.

Author Contributions

S.N.P.—Conceptualization, Writing—original draft, A.V.T.—Data curation, Editing, I.P.P., E.V.Z., J.A.B., Y.S.P.—Investigation.

Ethics Statement

Not applicable.

Informed Consent Statement

Not applicable.

Data Availability Statement

Data will be available on request.

Funding

This research was carried out with the financial support of the Russian Science Foundation, project (Agreement No. 21-73-30019-P).

Declaration of Competing Interest

The authors declare that they have no conflict of interest.

References

1. Böhler Welding. *Welding Materials for the Chemical and Petrochemical Industries*; Böhler Schweißtechnik Austria GmbH: Kapfenberg, Austria, 2008; 44p.
2. Reihani A, Haghighi RD. Failure analysis and weld ability improvement of 35% Cr–45% Ni heat resistant alloy. *Eng. Fail. Anal.* **2015**, *52*, 97–108.
3. Reihani A, Razavi SA, Abbasi E, Etemadi A. Failure analysis of welded radiant tubes made of cast heat-resisting steel. *J. Fail. Anal. Prev.* **2013**, *13*, 658–665.
4. Popova I, Oryshchenko A, Utkin YA, Petrov S, Tsemenko A. Study of heat resistance characteristics of metal of centrifugally cast tubes made from 45Cr32Ni43SiNb alloy and their welded joints at temperatures up to 1150° C: Part 1. The heat resistance characteristics of tubes at temperatures up to 1100° C. *Inorg. Mater. Appl. Res.* **2021**, *12*, 1459–1466.
5. Kondrat'ev SY, Ptashnik A, Anastasiadi G, Petrov S. Analysis of transformations of carbide phases in alloy 25Cr35Ni by the method of quantitative electron microscopy. *Met. Sci. Heat Treat.* **2015**, *57*, 402–409.
6. Voicu R, Andrieu E, Poquillon D, Furtado J, Lacaz J. Microstructure evolution of HP40-Nb alloys during aging under air at 1000 °C. *Mater. Charact.* **2009**, *60*, 1020–1027.
7. Rudskoy AI, Kondrat'ev SY, Anastasiadi GP, Oryshchenko AS, Fuks MD, Petrov SN. Transformation of the structure of refractory alloy 0.45C–26Cr–33Ni–2Si–2Nb during long-term high-temperature hold. *Met. Sci. Heat Treat.* **2014**, *55*, 517–525.
8. Barbabela GD, de Almeida LH, da Silveira TL, Le May I. Phase characterization in two centrifugally cast HK stainless steel tubes. *Mater. Charact.* **1991**, *26*, 1–7.
9. de Almeida Soares GD, de Almeida LH, da Silveira TL, Le May I. Niobium additions in HP heat-resistant cast stainless steels. *Mater. Charact.* **1992**, *29*, 387–396.
10. Abbasi M, Park I, Ro Y, Ji Y, Ayer R, Shim J. G-phase formation in twenty-years aged heat-resistant cast austenitic steel reformer tube. *Mater. Charact.* **2019**, *148*, 297–306.
11. Guo X, Ni Y, Gong J, Geng L, Tang J, Jiang Y, et al. Formation of G-phase in 20Cr32Ni1Nb Stainless Steel and its Effect on Mechanical Properties. *Acta Metall. Sini. (Eng. Lett.)* **2017**, *30*, 829–839.
12. Zabavicheva E, Petrov S, Kondrat'ev SY. Transformation of Niobium Carbide in Heat-Resistant Alloys Based on Fe–25Cr–35Ni at 900° C and 1150° C. *Met. Sci. Heat Treat.* **2024**, *65*, 605–612.
13. Kondrat'ev SY, Anastasiadi G, Rudskoy A. Nanostructure mechanism of formation of oxide film in heat-resistant Fe–25Cr–35Ni superalloys. *Met. Sci. Heat Treat.* **2015**, *56*, 531–536.
14. Rudskoi A, Kondrat'ev SY, Anastasiadi G, Tsemenko A. Mechanism of the Oxidation of Phases in Heat-Resistant Alloys of the Fe–25Cr–35Ni System. *Phys. Met. Metallogr.* **2021**, *122*, 275–285.
15. Kondrat'ev SY, Tsemenko A. Mechanism of Formation of Surface Protective Layer in Heat-Resistant HP40NbTu Alloys during High-Temperature Oxidation. *Met. Sci. Heat Treat.* **2024**, *66*, 177–192.